Journal of Power Sources 196 (2011) 3249–3254

Contents lists available at ScienceDirect

Journal of Power Sources

journal homepage: www.elsevier.com/locate/jpowsour

Short communication

Arc ion plated Cr/CrN/Cr multilayers on 316L stainless steel as bipolar plates for polymer electrolyte membrane fuel cells

Min Zhang [a,c,*], Bo Wu [b], Guoqiang Lin [b], Zhigang Shao [c], Ming Hou [c], Baolian Yi [c]

[a] School of Physics and Electronic Technology, Liaoning Normal University, Dalian 116029, China
[b] Lab of Material Modification by Laser, Ion, and Electron Beams, Dalian University of Technology, Dalian 116085, China
[c] Fuel Cell R&D Center, Dalian Institute of Chemical Physics, Chinese Academy of Sciences, Dalian 116023, China

ARTICLE INFO

Article history:
Received 16 October 2010
Received in revised form
29 November 2010
Accepted 29 November 2010
Available online 4 December 2010

Keywords:
Stainless steel bipolar plate
Arc ion plating
Multilayer
Interfacial contact resistance
Electrochemistry corrosion

ABSTRACT

Arc ion plating (AIP) is applied to coat sandwich-like Cr/CrN/Cr multilayers on stainless steel 316L (SS316L) as bipolar plates for polymer electrolyte membrane fuel cell (PEMFC). Phase structure, hardness, adhesion property, interfacial contact resistance (ICR) between bipolar plates and carbon papers, and electrochemical corrosion property in the simulated PEMFC conditions are investigated. Cr phase with crystal plane of (1 1 0), (2 1 1), (3 2 2), and CrN phase with (3 2 1) are observed in the multilayer. The coating is found smooth, continuous and dense in cross-sectional observation by SEM, and the sandwiched structure of the coating is also confirmed by EDX results. Scratch tests show that the multilayer exhibits strong adhesion strength with steel substrate, which is beneficial to prevent layers from peeling off mechanically. After the coating treatment, the performance of the bipolar plate is greatly improved. Knoop hardness of the bipolar plates increases from 324 HK to 692 HK. The ICR decreases by one order of magnitude; furthermore, the corrosion resistance was also enhanced. Our analysis indicates that the improvement is attributed to high adhesion force of the smooth and dense coating and the synergistic function of Cr/CrN/Cr multilayer structure.

1. Introduction

A polymer electrolyte membrane fuel cell has attracted increasing interests due to its high efficiency and near-zero emissions as a power source. Currently, the major challenges for the commercial application of PEMFC systems include reducing the cost and weight of the fuel cell stack. One of the key components of the fuel cell stack is the bipolar plate which has the main functions of distributing and separating the cathodic and anodic reactant gases, and collecting and transmitting electric current [1]. Good conductivity, high corrosion resistance, high mechanical strength, and low gas permeability, low cost and easy machining are highly desirable characteristics for ideal bipolar plates [2]. Stainless steel 316L exhibits most of the characteristics and is widely considered as a promising bipolar plate material [3]. However, its corrosion resistance is still far from satisfaction in the acidic environment of PEMFC operation. The corrosion products, such as Fe ions, tend to contaminate the catalysts and poison the proton exchange membrane, reducing the overall efficiency of the cell [4]. Meanwhile, the corrosion finally causes the formation of a passivating layer on the stainless steel surface, which leads to an increase in ICR and a decrease in cell performance [5]. Additionally, the corrosion can deteriorate water management in the fuel cell, leading to increased mass transport losses. These effects cause the durability of the fuel cells degrade quickly, resulting in a poor lifetime [6].

How to impart SS316L bipolar plates with sufficient corrosion resistance and contact conductivity inexpensively is currently a hot issue. Forming a protective film on the plates by surface modification is proven to be an effective method and has been extensively studied. Fu et al. reported that both CrN [7] and Cr_xN gradient films [8] on SS316L by arc ion plating show high interfacial conductivity and good corrosion resistance in 0.5 M H_2SO_4 + 5 ppm F^- solution. Subsequently, Carbon-based films coated SS316L bipolar plates were reported by Fu to enhance corrosion resistance and interfacial conductivity in simulated PEMFC conditions [9]. Good initial performance of PEMFC stacks assembled with $Cr_{0.5}N_{0.5}$ film coated bipolar plates was close to that of the cell assembled with the Ag-plated ones [10]. Lee and co-workers investigated the ICR and corrosion resistance of TiCrN and titanium oxynitride films on SS316L bipolar plates by magnetron sputtering [11]. The bipolar plates were also coated with Ni [12] and Cr [13] by electroplating. Wang conducted plasma nitriding on SS316L plates and found that the treated plates exhibit good corrosion resistance, however poor interfacial conductivity [14]. Brady used thermal nitridation to form

* Corresponding author at: School of Physics and Electronic Technology, Liaoning Normal University, No. 850 Huanghe Road, Shahekou District, Dalian 116029, China. Tel.: +86 411 84379117; fax: +86 411 84379185.
E-mail address: m.zhang@live.com (M. Zhang).

0378-7753/$ – see front matter © 2010 Elsevier B.V. All rights reserved.
doi:10.1016/j.jpowsour.2010.11.154

a pin-hole free nitride layer on metallic bipolar plates, including Ni–Cr based alloys [15,16], Fe–Cr based alloys [17], AISI446 [18], and 349™ [19]. It was found that dense Cr nitride layer formed on Ni–Cr based alloys and exhibited improved corrosion resistance and low ICR under simulated PEMFC conditions, while thermal nitrided 349™ showed poor corrosion resistance because of the lack of continuity of the Cr-rich nitride layer [19]. Additionally, thermal nitrification generally requires a high-temperature process (>1000 °C) that can cause undesirable deformation of the machined metal bipolar plate [20] and a decrease of corrosion resistance [21]. Further, the process typically entails a high manufacturing cost.

More recently, Wang et al. [22] investigated the performance of TiN-, TiAlN- and CrN-coated SS316L bipolar plates by EBPVD under simulated PEMFC environments. It was found that CrN-coated SS316L showed a significantly lower ICR and better corrosion resistance. They suggested that multilayered coatings may disconnect the pinholes, or prevent through-coating pinholes and block corrosion channels. Zhang et al. [23] also deduced that a Ti_2N/TiN multilayer coating can provide superb corrosion protective layer for stainless steel. Despite of this, few reports have been presented on the possibility of the multilayer used for PEM fuel cell bipolar plates, maybe due to complicated process and poor cost efficiency.

Arc ion plating has been widely used to form efficiently protective coatings on cutting tools, dies, and bearings, etc. It is one of the most cost-efficient and economic deposition processes among PVD techniques. According to our previous study [8,24,25], arc ion plating, applying a pulsed substrate bias, PBAIP in short, inherits the advantages of arc ion plating, such as high ionized degree, high deposition rate and strong bonging strength, etc. More importantly, a pulsed bias brings new features in this conventional PVD technique, such as reduced droplets, dense films and low-temperature deposition. As a result, films with excellent performance can most likely be obtained. In addition, PBAIP is an environment-friendly process.

In this study, a sandwich-like Cr/CrN/Cr multilayer was designed and deposited on SS316L substrates as bipolar plates in PEMFCs by pulsed bias arc ion plating (PBAIP). Coating quality was evaluated by morphology, phase structure, film hardness, adhesion strength using XRD, SEM, micro-hardness and scratch tests. The interfacial contact resistance (ICR) and anti-corrosion property in the simulated PEMFC environments was presented as well.

2. Design of materials and coating structure

Cr is a kind of inexpensive and abundant metal with a good electrical conductivity and chemical stability. Cr-based coatings can help reduce the production cost. Bare Cr coating has poor mechanical and anti-corrosion properties, while CrN is a conductive nitride with good mechanical and anti-corrosion properties. The combination of Cr and CrN is of great potential to exhibit the synergistic functions. It was found in many reports [11,22,23,26–28] that the ICR decreases with increase in the compaction force. Choi et al. pointed out that this influence of the compaction force is due to an enlargement of the actual contact area under an increasing compaction force [11], and Lee et al. [29] also stated that an increase in the contact areas acts as electrical junctions, leading to an decline of ICR. Soft metal, like Cr, will help increase contact area when pressed, so Cr layer was selected as the outmost layer. Then CrN was assigned as the underneath layer to enhance the mechanical and anti-corrosion property. Accounting for higher internal stress usually caused by the big dismatch of physical properties between hard ceramic CrN and relative soft metallic SS316L [30,31], an interlayer of Cr followed CrN layer to improve the bonding strength. So the designed coating was sandwich-like structure, i.e. Cr/CrN/Cr multilayer.

3. Experimental methods

Bulat-6 arc ion plating system was used in this study. Two opposite Cr targets, 99.9% pure and 55 mm in diameter, were mounted at the end of linear ducts that connect to the chamber. Both ducts consisted of a two-step magnetic coil. The first-step coil was used to stabilize the burning arc, and the second-step one was used to constrain the plasma and remove some droplets. Stainless steel holders lying in the middle of the plasma beams can rotate and turn simultaneously. The distance between the centre of the holder and the arcs was 600 mm. A pulsed bias was applied on the holders through the axis.

Stainless steel 316L was chosen as the base metal of bipolar plates. The stainless steel substrates with size of 100 mm × 100 mm × 0.1 mm were ultrasonically cleaned in acetone, ethyl ethanol and deionized water for 15 min. Then they were blown dry and put on holders. The chamber was evacuated to a base pressure below 5.0×10^{-3} Pa using a turbo molecular pump and a rotary pump. Prior to the deposition, the substrates were sputtered by Ar ions for 10 min with a pulsed bias of −800 V in ambient Ar at 2.0 Pa.

When the deposition began, two Cr targets were burnt by the triggers, and both arc currents were kept at 80 A. The partial pressure of Ar was kept at 0.5 Pa. The bias voltage, frequency and duty cycle of the pulsed bias were −300 V, 20 kHz and 40%, respectively. 10 min later, nitrogen gas was introduced in the chamber by mass flow meter and the flow rate was 102 sccm. After 20 min of CrN deposition, the flow rate of N_2 decreased immediately to zero. The deposition process preceded another 10 min, and then halted. According to the deposition rate of our AIP system, the thickness of Cr and CrN layer was controlled to 0.25 and 0.5 μm, consistent with our design.

Phase structure was detected with XRD-6000 X-ray diffractor. Film hardness was measured with a DMH-2LS Knoop hardness tester. Morphology of cross-section and scratch track was observed with scanning electron microscopy (JSM-5600LV). Adhesion strength was evaluated with a CSR-01 scratch tester.

The ICR between uncoated, coated bipolar plates and diffusion layer (carbon paper) was measured with the method similar to that reported by Wang et al. [3]. In the setup, two pieces of Toray carbon paper were sandwiched between the bipolar plate sample and two copper plates. The copper plates were plated with gold on both sides to enhance conductivity. An electrical current of 5.0 A, sourced by a PSP-2010 programmable power supply, was provided via the two copper plates. During the tests, the compacting force was increased gradually at a step of $5\ N\ s^{-1}$ controlled by a WDW electromechanical universal testing machine.

Corrosion behaviors of the samples were investigated by polarization electrochemical experiments using a potentiostat Model 2273A by EG&G Princeton Applied Research and analyzed with the corrosion software of EG&G Version 2.43.0. To simulate an aggressive PEMFC environments, a 0.5 M H_2SO_4 + 2 ppm F^- solution at 70 °C was used, bubbled thoroughly with either hydrogen gas (simulating a PEMFC anodic environment) or pressured air (simulating a PEMFC cathodic environment) prior to and during the electrochemical tests. A conventional three-electrode system was used in the electrochemical measurements, in which a platinum sheet acted as the counter electrode, a saturated calomel electrode (SCE, sat'd KCl) as the reference electrode and the stainless steel sample as the working electrode. The size of the working electrodes prepared was 15 mm × 15 mm × 0.1 mm. The edges were sealed by insulating epoxy resin, only leaving a 10 mm × 10 mm surface exposed to the electrolyte. A copper wire was soldered to the backside of the sample for ohmic contact. As for the potentiodynamic polarizations, the samples were stabilized at open circuit potential (OCP)

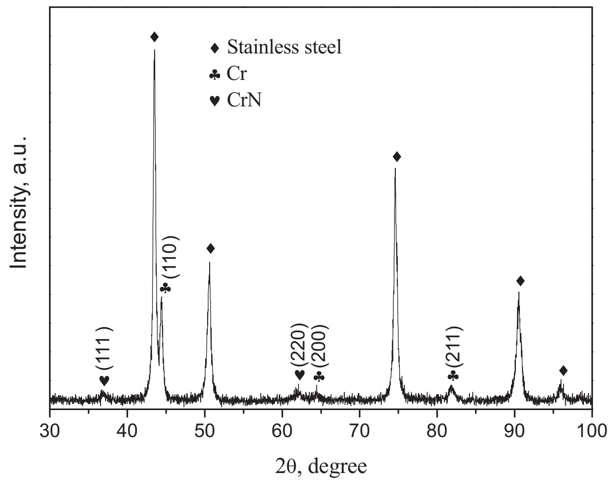

Fig. 1. XRD pattern of Cr/CrN/Cr multilayer.

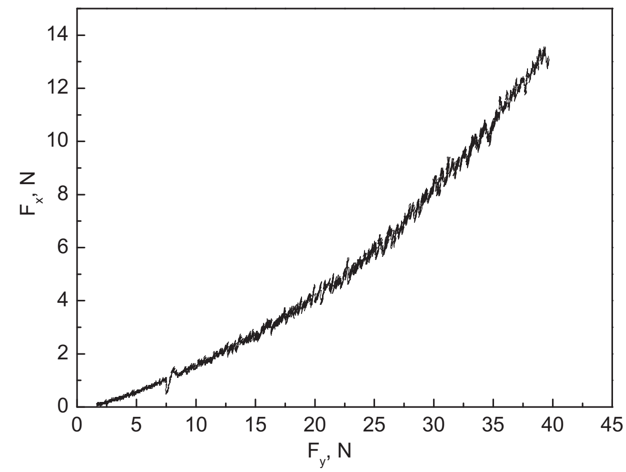

Fig. 3. Scratch test curve of the Cr/CrN/Cr multilayer.

for 10 min, and then the potential was swept from the OCP in the anodic direction at a scanning rate of 20 mV s^{-1}.

In order to evaluate the stability of the samples in the actual working conditions of PEMFC, potentiostatic polarizations were performed for over 6 h. During the measurements, the specimens were also stabilized at open circuit for 10 min. The current density as a function of time were recorded at applied anode (−0.1 V) and cathode (+0.6 V) potentials for PEMFC.

4. Results

4.1. Coating characterization

XRD pattern of Cr/CrN/Cr multilayer is shown in Fig. 1. Apart from the diffraction peaks from SS316L, diffraction peaks by the plane of Cr(1 1 0), (2 0 0), (2 1 1), CrN(1 1 1) and (2 2 0) are observed. It can be concluded that the coating consist of Cr and CrN phases.

Fig. 2(a) shows the cross-sectional SEM image of the multilayer. To increase the contract, a slight corrosion with chloroazotic acid solution was exerted on the cross-section of the coating. The multilayer appears 1.0–1.2 μm thick, dense, continuous, and no microcrack and void are observed, suggesting that the film exhibits good corrosion resistance. An EDX line scanning curve of N element was performed along a minor distance indicated by the inset arrow in Fig. 2(a), via which a relative content of N can be obtained. The EDX result is presented in Fig. 2(b). It is obvious that there is an N-rich peak oCcurring at 0.5 μm inward from the film surface, where is the midst of film thickness. Combining with XRD results, it can be concluded that it is corresponding to CrN layer, which is the middle layer of the sandwich-like Cr/CrN/Cr multilayer. The as-deposited film conforms well to our design.

Adhesion force is an important indicator of film quality, especially for bipolar plates in PEMFCs, because good adhesion property is desirable to prevent peeling off during assembly process of fuel cell stacks. Scratch test is a widely used to evaluated adhesion force of the coatings. A Rockwell diamond is pulled across the sample with an increasing normal load, F_y. Accordingly, a horizon force, F_x, is applied to make the pin move at a constant translation speed. When the pin punctuates through the coating, the coating will peel off, meanwhile the horizon force will increase significantly, a break point will occur on the curve of F_x vs. F_y. The value of the normal load is identified as adhesion force of the coating. Fig. 3 shows the scratch curve of the Cr/CrN/Cr multilayer, and we can see that the horizon force increases with the normal load. In the full range of test, we cannot see any break point, indicating that the coating did not fail even when subjected to the maximum normal load.

Fig. 4 presents the SEM images of a scratch track. It can be seen in Fig. 4(a) and (b) that the toughness of the coating is good and no peeling-off occurs along the whole track. As shown in Fig. 4(c) and (d), just a little wrinkle piled on both sides of the track, and a cavity occurs at the end of track indicated by the inset white cycle. It can be concluded that the Cr/CrN/Cr multilayer exhibits good toughness and adhesion property, which is attributed to good toughness of both Cr layers and bonding function of the Cr interlayer. Thus it would be induced that adhesion property of CrN-coated samples would not be so good, because of the absence of the Cr interlayer.

Knoop hardness test was performed to evaluate the hardness of the coated SS316L bipolar plate. The hardness of uncoated and

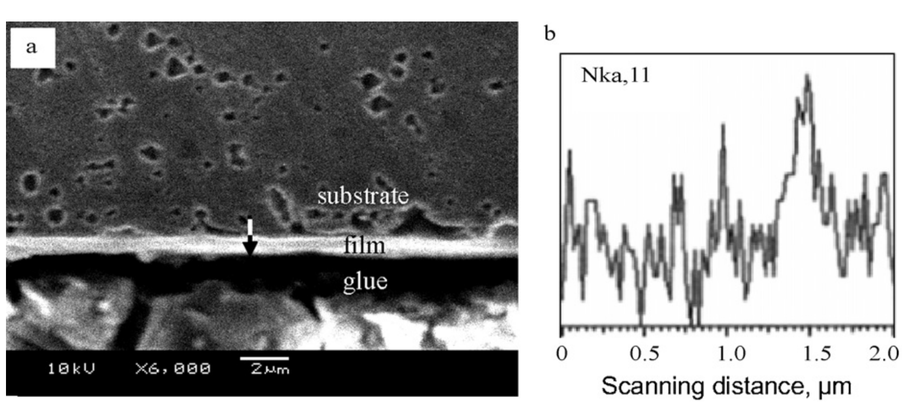

Fig. 2. Cross-sectional SEM image of the Cr/CrN/Cr multilayer (a) and line scanning curve (b) of N element.

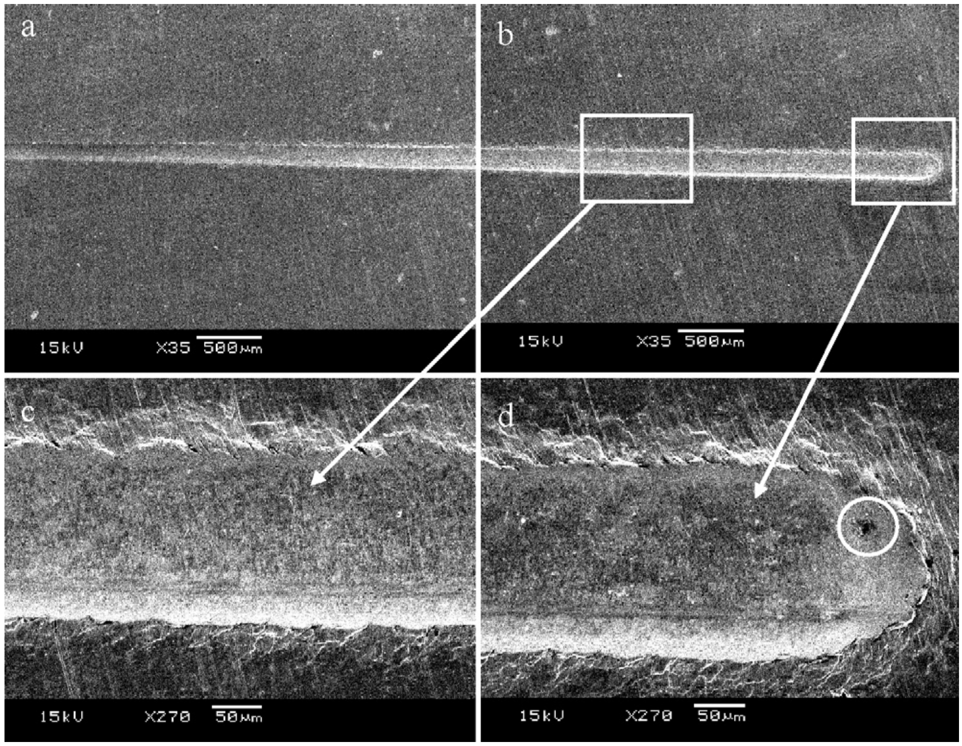

Fig. 4. SEM images of the scratch track.

Cr/CrN/Cr multilayer coated SS316L bipolar plate is presented in Table 1. We can see that the hardness of bipolar plate increases from 324 HK for the uncoated samples to 692 HK for the coated ones, which is helpful to resist the shock and wear during assembly process of fuel cell stacks.

4.2. Corrosion testing

The potentiodynamic curves of the coated and uncoated SS316L bipolar plate samples are shown in Fig. 5. From the slopes of the anodic curve and the cathodic curve, the corresponding corrosion current can be determined by Tafel mothod. Compared with that of the bare SS316L, corrosion current density of the Cr/CrN/Cr multilayer coated SS316L decreases from $10^{-4.2}$ to $10^{-5.4}$ A cm^{-2} for the anodic environment, and from $10^{-4.6}$ to $10^{-5.9}$ A cm^{-2} for the cathodic environment. That is to say, corrosion current density of the coated sample is one order of magnitude lower than that of SS316L substrate. Additionally, the OCP of the coated sample keeps higher than that of the bare SS316L under both anodic and cathodic conditions. Thus it can be concluded that the Cr/CrN/Cr coated samples exhibit better corrosion resistance than the bare SS316L.

Fig. 6 presents the current density measured as a function of time from the potentiostatic polarization. It can be seen in Fig. 6(a) that the corrosive current density of the coated sample in simulated anodic condition stabilizes in the range of 10^{-6} A cm^{-2}–$10^{-6.25}$ A cm^{-2}, about two orders of magnitude lower than that of the bare SS316L, around $10^{-4.3}$ A cm^{-2}. From Fig. 6(b), we can see that the corrosive current density of the coated sample in simulated anodic condition maintains at $10^{-6.5}$ A cm^{-2}, still lower than that of the bare SS316L, in the range of $10^{-6.6}$ A cm^{-2}–$10^{-6.8}$ A cm^{-2}. The results obtained in both anodic and cathodic conditions imply that coated with Cr/CrN/Cr, the SS316L bipolar plate has better long-term stability in simulated PEMFC environments.

In short, the corrosion resistance of the SS316L bipolar plates is enhanced by coating a Cr/CrN/Cr multilayer using pulsed bias arc ion plating.

Table 1
Knoop hardness of uncoated and coated SS316L bipolar plates.

Sample	Uncoated	Cr/CrN/Cr coated
Knoop hardness, HK	324	692

4.3. Interfacial contact resistance

ICRs between the samples and carbon paper under a compaction pressure ranging from 15 to 195 N cm^{-2} are shown in Fig. 7. The red and black line in Fig. 7 shows the dependence of ICR of the uncoated and Cr/CrN/Cr coated SS316L samples on the compaction pressure, respectively. With increasing compaction pressure, the resistance of the materials decreases rapidly at a low compaction pressure range (<40 N cm^{-2}) and then decreases gradually at higher compaction pressures. The uncoated sample has a much higher contact resistance than the coated one, which can be attributed to the natural oxide layer on the steel surface. Under a compaction pressure of 150 N cm^{-2}, the ICR of the coated sample falls in the range from 30 to 35 mΩ cm^2, close to the DOE 2010 target of <20 mΩ cm^2. Additionally, the resistance of the coated sample is one order of magnitude lower than that of the uncoated sample, indicating Cr/CrN/Cr multilayer plays a crucial role in reducing the ICR.

The blue and green line in Fig. 7 shows the ICRs of the coated SS316L samples after potentiostatic polarization testing for over 6 h in the simulated cathodic and anodic environments, respectively. After potentiostatic polarization in either simulated cathodic or anodic environment, the ICR of the Cr/CrN/Cr coated sample gets higher in comparison with that before testing. At 145 N cm^{-2} compaction force, the ICR of the coated sample in simulated cathodic and anodic environment increases from 35 mΩ cm^2 to 60 mΩ cm^2 and 80 mΩ cm^2, respectively.

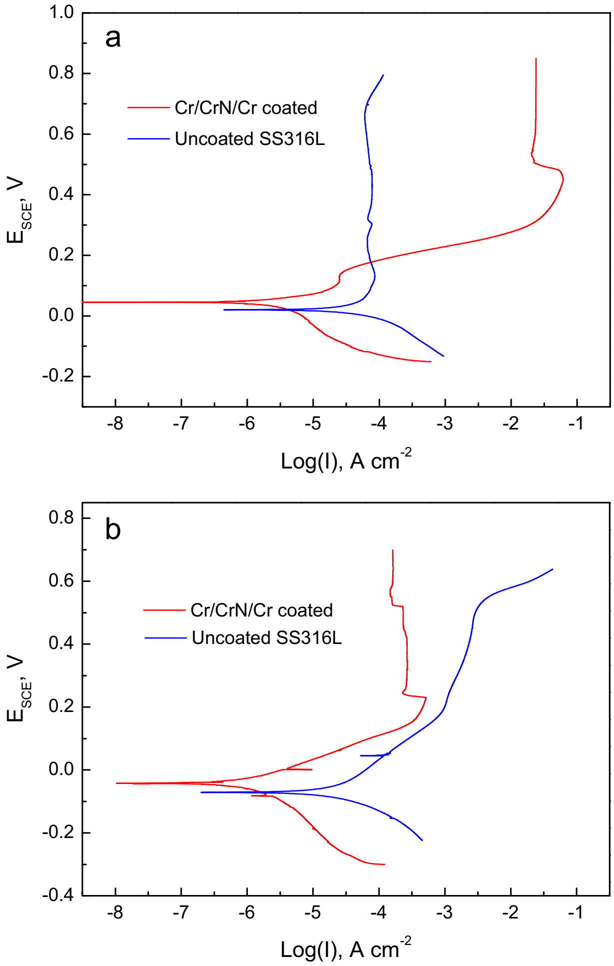

Fig. 5. Potentiodynamic polarization curves of the uncoated and coated samples in 0.5 M H_2SO_4 with 2 ppm F^- at 70 °C (a) H_2 bubbling for the anodic condition and (b) air bubbling for the cathodic condition.

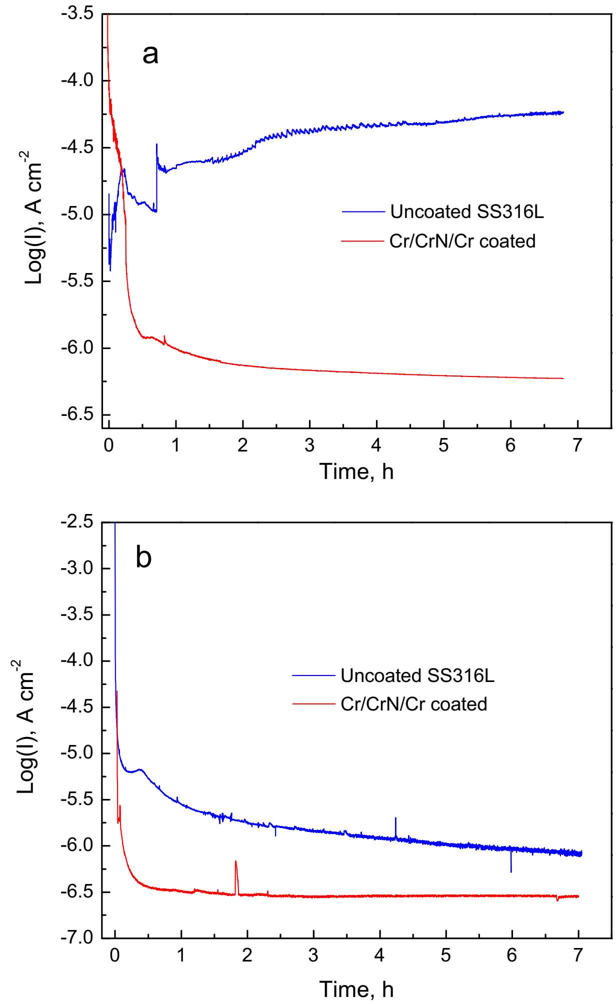

Fig. 6. Potentiostatic polarization curves of the uncoated and coated samples in 0.5 M H_2SO_4 with 2 ppm F^- at 70 °C (a) H_2 bubbling at −0.1 V_{SCE} and (b) air bubbling at 0.6 V_{SCE}.

5. Discussions

The performance of SS316L bipolar plates coated with Cr/CrN/Cr multilayer were greatly improved, which is close relating to the microstructure and material nature of the multilayer. In both PEMFC anode and cathode environments, SS316L underwent passivation, forming a passive film, and the ICR between the steel and the carbon backing material increased due to passive film formation. On the other hand, the passive film may not protect the bipolar plate from further corrosion in the fuel cell environment, and the corrosion product could poison the catalysts and decrease the efficiency of the cell. It hinders the wide application of SS316L in PEMFCs.

In this study, the outmost layer of the multilayer is Cr, which exhibits good conductivity and corrosion resistance. Under a certain compact force, the soft nature of Cr will results in a very dense contact with MEA, which will facilitate to reduce the ICR. The CrN layer plays a crucial role in the overall corrosion resistance. Even corrosion channels puncture throughout the outmost Cr layer, CrN layer can effectively block corrosion frontiers, slower the corrosion process, and as a result, the anti-corrosion property is greatly improved. It could be certain that little Cr ions will dissolve from the outmost Cr layer, which is unfavorable for PEMFC efficiency and lifetime. To avoid this problem, the outmost layer will alter to be some conductive nitride layer, instead of a pure metal layer, in our subsequent work. Furthermore, the multilayer structure, such as every single-layer thickness, will be optimized to get a cost-effective coating, on the basis of the optimization of deposition parameters to eliminate the defects like macroparticles and pin-holes to the utmost in every single layer. Despite of this, the Cr/CrN/Cr multilayer obtained in this study can be cost-effective

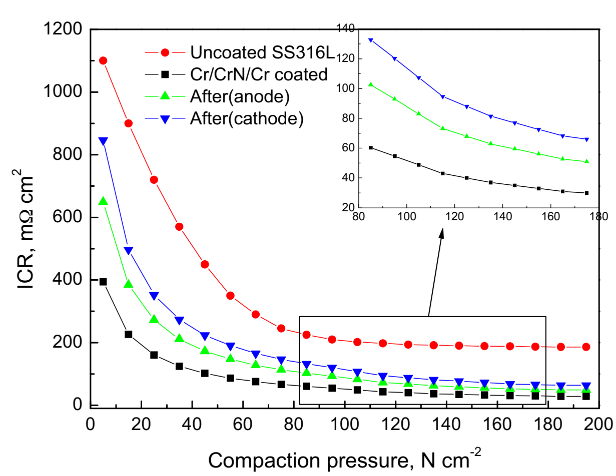

Fig. 7. ICRs as a function of compaction pressure of uncoated, Cr/CrN/Cr coated SS316L samples, and the coated samples after potentiostatic polarization testing for over 6 h in the simulated cathodic and anodic environments.

due to some features of AIP process applied in this work, such as batch treatment, simply operation for multilayer synthesis, and low cost of raw materials like Cr targets, argon and nitrogen gas.

The property enhancement of coated bipolar plate is relating to coating quality as well. Among ion plating techniques, arc ion plating used in this study exhibits highest ion rate [32,33]. Applying a pulsed substrate bias can effectively accelerate the ions and result in ion bombardment on the surface of the forming film [24]. The bombardment effect facilitates to form a dense and uniform film, but also to form a pseudo-diffusion layer at the layer-to-layer interfaces of the multilayers, which reduces interfacial electrical resistance and crystalline defects [34]. Argon ion sputtering clean, prior to the deposition process, can remove the passivation layer on stainless steel substrates, enhance surface reactivity, and resultantly increase bonding strength. These features of arc ion plating facilitate to form a dense, smooth and less defective film with a strong bonding strength.

According to the aforementioned results and discussion, it is feasible that SS316L coated with Cr/CrN/Cr multilayer by arc ion plating can be used as bipolar plates for fuel cell applications. These preliminary results are encouraging however the properties of bipolar plates coated with Cr/CrN/Cr multilayer still need to be further improved. For instance, the ICR obtained in this study decreases by one order of magnitude, but there is a long way to go to reach the ideal ICR value of $\leq 20\,\mathrm{m}\Omega\,\mathrm{cm}^2$. It is believed that the corrosion property and contact resistance of SS316L bipolar plates can be further enhanced by a better understanding of the corrosion mechanisms and optimization of the coating composition and structure for PEMFC bipolar plate application.

6. Conclusions

Cr/CrN/Cr multilayer with good quality was fabricated on SS316L bipolar plate by arc ion plating. The performance of the coated samples was greatly improved. Compared with the bare SS316L bipolar plate, the plates coated with Cr/CrN/Cr multilayer exhibit superior corrosion resistance and lower ICR. The enhancement of the performance is attributed to the high adhesion force of the smooth and dense coating and the synergistic function of Cr/CrN/Cr multilayer structure. Arc ion plating a multilayer is a promising approach worthwhile exploring to improve the corrosion resistance and conductivity of SS316L bipolar plates under PEMFC application conditions.

Acknowledgement

The author, M. Zhang, thanks Dr. Huabing Zhang for her kind help in electrochemical experiments. This work was financially supported by the National High Technology Research and Development Program of China (863 Program, no. 2007AA03Z221).

References

[1] B. Yi, Fuel Cells—Principle, Technology and Application, 1st ed., Chemical Industry Press, Beijing, 2003.
[2] A. Hermann, T. Chaudhuri, P. Spagnol, International Journal of Hydrogen Energy 30 (2005) 1297–1302.
[3] H. Wang, M.A. Sweikart, J.A. Turner, Journal of Power Sources 115 (2003) 243–251.
[4] M.J. Kelly, G. Fafilek, J.O. Besenhard, H. Kronberger, G.E. Nauer, Journal of Power Sources 145 (2005) 249–252.
[5] H. Tawfik, Y. Hung, D. Mahajan, Journal of Power Sources 163 (2007) 755–767.
[6] C.Y. Chung, S.K. Chen, T.S. Chin, T.H. Ko, S.W. Lin, W.M. Chang, S.N. Hsiao, Journal of Power Sources 186 (2009) 393–397.
[7] Y. Fu, G. Lin, M. Hou, B. Wu, H. Li, L. Hao, Z. Shao, B. Yi, International Journal of Hydrogen Energy 34 (2009) 453–458.
[8] Y. Fu, M. Hou, G. Lin, J. Hou, Z. Shao, B. Yi, Journal of Power Sources 176 (2008) 282–286.
[9] Y. Fu, G. Lin, M. Hou, B. Wu, Z. Shao, B. Yi, International Journal of Hydrogen Energy 34 (2009) 405–409.
[10] B. Wu, Y. Fu, J. Xu, G. Lin, M. Hou, Journal of Power Sources 194 (2009) 976–980.
[11] H.S. Choi, D.H. Han, W.H. Hong, J.J. Lee, Journal of Power Sources 189 (2009) 966–971.
[12] S.A.A. El-Enin, O.E. Abdel-Salam, H. El-Abd, A.M. Amin, Journal of Power Sources 177 (2008) 131–136.
[13] D.-G. Nam, H.-C. Lee, Journal of Power Sources 170 (2007) 268–274.
[14] R. Tian, J. Sun, L. Wang, International Journal of Hydrogen Energy 31 (2006) 1874–1878.
[15] M.P. Brady, K. Weisbrod, I. Paulauskas, R.A. Buchanan, K.L. More, H. Wang, M. Wilson, F. Garzon, L.R. Walker, Scripta Materialia 50 (2004) 1017–1022.
[16] I.E. Paulauskas, M.P. Brady, I.H.M. Meyer, R.A. Buchanan, L.R. Walker, Corrosion Science 48 (2006) 3157–3171.
[17] M. Brady, H. Wang, B. Yang, J. Turner, M. Bordignon, R. Molins, International Journal of Hydrogen Energy 32 (2007) 3778–3788.
[18] H. Wang, M. Brady, K. More, I.H. Meyer, J. Turner, Journal of Power Sources 138 (2004) 79–85.
[19] H. Wang, M.P. Brady, G. Teeter, J.A. Turner, Journal of Power Sources 138 (2004) 86–93.
[20] E.S.P. Cabrera, Materials Science and Technology 17 (2001) 155–161.
[21] P.A. Dearnley, A. Namvar, T. Bell, Plasma Surface Engineering 1 (1989) 219–226.
[22] L. Wang, D.O. Northwood, X. Nie, J. Housden, E. Spain, A. Leyland, A. Matthews, Journal of Power Sources 195 (2010) 3814–3821.
[23] D. Zhang, L. Duan, L. Guo, W.-H. Tuan, International Journal of Hydrogen Energy 35 (2010) 3721–3726.
[24] M. Zhang, G. Lin, C. Dong, L. Wen, Surface and Coatings Technology 201 (2007) 7252–7258.
[25] M.D. Huang, Y.P. Lee, C. Dong, G.Q. Lin, C. Sun, L.S. Wen, Journal of Vacuum Science & Technology A: Vacuum Surfaces and Films 22 (2004) 250–256.
[26] A. Afshar, M. Yari, M.M. Larijani, M. Eshghabadi, Journal of Alloys and Compounds 502 (2010) 451–455.
[27] S.Y. Kim, D.H. Han, J.N. Kim, J.J. Lee, Journal of Power Sources 193 (2009) 570–574.
[28] J. Barranco, F. Barreras, A. Lozano, A.M. Lopez, V. Roda, J. Martin, M. Maza, G.G. Fuentes, E. Almandoz, International Journal of Hydrogen Energy 35 (2010) 11489–11498.
[29] W.G. Lee, K.H. Cho, S.B. Lee, S.B. Park, H. Jang, Journal of Alloys and Compounds 474 (2009) 268–272.
[30] M. Zhang, M.K. Li, H.K. Kim, F. Pan, Applied Surface Science 255 (2009) 9200–9205.
[31] D.S. Kang, J.T. Ok, S.J. Heo, E.Y. Choi, M.C. Kang, K.H. Kim, Solid State Phenomena 118 (2006) 281–286.
[32] W. Olbrich, J. Fessmann, K.G. Ebberink, Journal of Surface Coating & Technology 49 (1991) 258–262.
[33] R.L. Boxman, V.N. Zhitomirsky, Review of Scientific Instruments 77 (2006) 1–15.
[34] Y. Zhao, PhD Dissertation in Material Science & Engineering, Dalian University of Technology, Dalian, 2006.